Optimization of breast cancer detection in Dual Energy X-ray Mammography using a CMOS imaging detector

V Koukou[1], G Fountos[2], N Martini[1], P Sotiropoulou[1], C Michail[2], N Kalyvas[2], I Valais[2], A Bakas[3], E Kounadi[4], I Kandarakis[2] and G Nikiforidis[1]

[1] Department of Medical Physics, Medical School, University of Patras, 265 00 Patras, Greece
[2] Department of Biomedical Engineering, Technological Educational Institute of Athens, Egaleo, 122 10 Athens, Greece
[3] Department of Medical Radiologic Technology, Technological Educational Institute of Athens, Egaleo, 122 10 Athens, Greece
[4] Ministry of Health, SEYYP, Pireos 205, 11853, Athens, Greece

E-mail: gfoun@teiath.gr

Abstract. Dual energy mammography has the ability to improve the detection of microcalcifications leading to early diagnosis of breast cancer. In this simulation study, a prototype dual energy mammography system, using a CMOS based imaging detector with different X-ray spectra, was modeled. The device consists of a 33.91 mg/cm^2 Gd_2O_2S:Tb scintillator screen, placed in direct contact with the sensor, with a pixel size of 22.5 μm. Various filter materials and tube voltages of a Tungsten (W) anode for both the low and high energy were examined. The selection of the filters applied to W spectra was based on their K-edges (K-edge filtering). Hydroxyapatite (HAp) was used to simulate microcalcifications. Calcification signal-to-noise ratio (SNR_{tc}) was calculated for entrance surface dose within the acceptable levels of conventional mammography. Optimization was based on the maximization of SNR_{tc} while minimizing the entrance dose. The best compromise between SNR_{tc} value and dose was provided by a 35kVp X-ray spectrum with added beam filtration of 100μm Pd and a 70kVp Yb filtered spectrum of 800 μm for the low and high energy, respectively. Computer simulation results show that a SNR_{tc} value of 3.6 can be achieved for a calcification size of 200 μm. Compared with previous studies, this method can improve detectability of microcalcifications.

1. Introduction

Screening and diagnosis using X-ray mammography rely on the early detection of microcalcifications (μCs) and soft-tissue masses [1-4]. The detection and visualization of μCs are often obscured by the overlapping tissue structures. Dual-Energy (DE) imaging technique offers an alternative approach for imaging and visualizing μCs . With this technique, high- and low-energy images are acquired and their differences are used to cancel out the background tissue structures. In the resulting subtracted image,

'signal' is the difference of the means between a target and its background, and 'noise' is the standard deviation of that difference. The SNR is the ratio between signal and noise [1]. For the dual-kVp technique, the SNR depends, among other factors, on the energy spectrum of the original low- and high-energy X-ray beams, the elemental composition of the objects in the image and the efficiency of the image receptor [2].

SNR in DE subtracted images is a powerful parameter to predict the visibility of the detail of interest against the background after the subtraction. Generally, the SNR in the subtracted images will be lower than in the original ones [3]. *Shaw and Gur* analyzed the SNR for various techniques of dual-energy subtraction and concluded that for the dual-kVp method, the SNR in the subtracted image would generally increase as the difference in kVp between the low and the high-energy exposures maximized [3]. *Lemacks et al* presented a numerical framework to calculate the signal-to-noise ratio of the subtracted microcalcification (μC) image for dual-kVp subtraction, and applied it to polyenergetic beams [4]. Their results applicable to Mo/Mo and W/La (anode/filter) beams, showed that for a 5cm thick compressed breast composed of 50% glandular and 50% adipose tissue, a SNR of 3 was achieved for a μC size of 250 μm, for certain combinations of low- and high-energy exposures [4]. However, under the current implementations of Dual Energy Digital Mammography (DEDM) the minimum detectable microcalcification size is in the range of 250 μm and 355 μm [4-8].

In this simulation study, a prototype dual energy mammography system using a CMOS based imaging detector with different X-ray spectra was modeled. The aim of the present study is the detection of the minimum microcalcification size for entrance surface dose within the acceptable levels of conventional mammography. Calcification signal-to-noise ratio (SNR_{tc}) was calculated and optimization was based on the maximization of SNR_{tc} while minimizing the entrance dose. Also, monochromatization of the X-ray spectra with the use of K-edge filtering technique was included.

2. Materials and Methods

An analytical model was developed in order to determine the calcification SNR assuming only Poisson distribution [4]. The breast is composed of adipose tissue of thickness t_a, glandular tissue of thickness t_b, and a cubic microcalcification of thickness t_c.

Considering that polyenergetic X-rays are used, the mean measured signals in the low- and high-energy images, S_l and S_h, can be expressed as:

$$S_{l,h} = \int dE \times R_j \times d^2 \times \Phi_j(E) \times e^{-\frac{\mu}{\rho}\alpha(E)\rho_a t_a - g_r\left(\frac{\mu}{\rho}g\rho_g - \frac{\mu}{\rho}a\rho_a\right)T - \frac{\mu}{\rho}c(E)\rho_c t_c} \times A(E) \times Q(E) \quad (1)$$

The SNR of the subtracted signal, t_c, can be expressed as follows [4]:

$$SNR_{tc} = \frac{tc}{\sqrt{\sigma_{tc}^2}} \quad (2)$$

where σ_{tc} represents the noise level in the calcification subtraction image.

The unfiltered spectra were parameterized by Boone *et al* for a Tungsten (W) anode for both low and high energy [9,10]. The maximum tube voltage range was 23-35kVp for the low energy (LE) and 50-70kVp for the high energy (HE). The beams have been attenuated by various filters according to their K-edge (K-edge filtering) from 18keV to 61keV [11]. The filter thicknesses varied from 100-1000 μm for both energies.

The surface dose, after filtration of the X-ray beams, was calculated according to equation (3) [12]. The total exposure is the sum of the low- and high-energy exposures. So the whole process was adapted to all, low- and high-, kVp spectra from the Tungsten (W) anode.

$$Dose(mGy) = 1.83 \cdot 10^{-6} \cdot \Phi_o(E) \cdot E \cdot \left(\frac{\mu_{en}}{\rho} \right)_{air} \cdot 8.77 \cdot 10^{-3} \quad (3)$$

where $\Phi_o(E)$ is the filtered X-ray spectrum value (photons/mm^2) at energy E. μ_{en}/ρ is the X-ray mass energy absorption coefficient of air at energy E obtained from NISTIR (National Institute of Standards and Technology Interagency Report) [13].

The SNR has been evaluated for the subtracted digital images of 5cm thick compressed breast, with composition of 50% glandular and 50% adipose tissue. The microcalcifications tested, were 100, 150, 200, 250 and 300 μm thick [14].

The elemental compositions of adipose and glandular breast tissue, the microcalcifications, and the scintillator (Gd_2O_2S:Tb) were used to calculate the mass-attenuation coefficients using data published by NISTIR with the computer program XMuDat [13,15]. Hydroxyapatite (HAp) was used to simulate microcalcifications. Hydroxyapatite is a calcium-phosphate mineral form ($Ca_{10}(PO_4)_6(OH)_2$) and in crystalline form has a density of 3.18gr/cm^3 [16].Note that, in the calculation of SNR_{tc}, the mass attenuation coefficients were then replaced by *effective mass attenuation coefficients*.

In this study, terbium-doped gadolinium oxysulfide (Gd_2O_2S:Tb) was considered to be the scintillator material coupled to a CMOS photodiode pixel array (RadEye HR). This scintillator was selected due to its efficiency and imaging properties, which are superior in comparison to other detectors [17]. The density of Gd_2O_2S:Tb is 7.34 g/cm^3. The surface density, W, (density multiplied by the thickness of the material) of Gd_2O_2S:Tb used in this study is 0.03394 g/cm^2 (approximately 34 mg/cm^2). The sensor pitch is 22.5 μm. The Quantum Detection Efficiency (QDE), $A(E)$, and the matching factor (α_s), $Q(E)$, were calculated according to Michail *et al* [18].

Computer simulations provided values for the following parameters: (i) mean energy (ME), (ii) Full Width at Half Maximum (FWHM) and (iii) total entrance surface dose. Optimization was based on the minimization of total entrance surface dose, while maintaining SNR_{tc} above the threshold. The SNR_{tc} threshold was set to be 3 ($SNR_{tc} \geq 3$) [4]. Furthermore, minimization of FWHM leading to narrow energy band X-rays was included.

3. Results and Discussion

For low energy filter selection, FWHM was plotted as a function of surface density (density multiplied by the thickness of the material) for all low energy filters tested (Figure 1). Palladium (Pd) filter has the lower values of FWHM in the whole surface density range, leading to narrower spectra. For this reason, Pd was selected as the low energy filter.

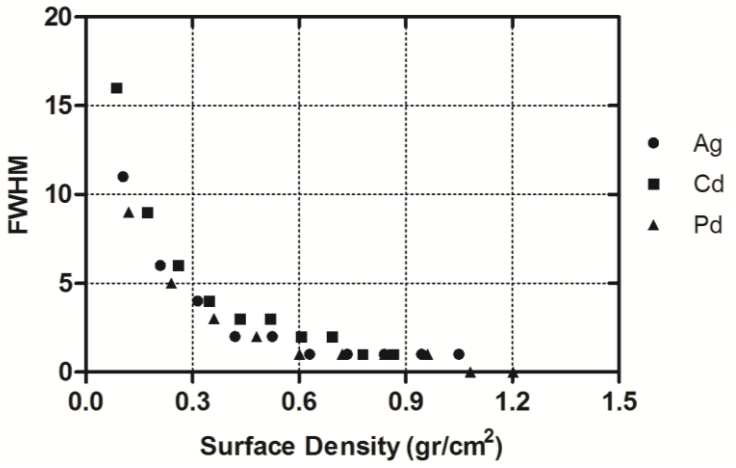

Figure 1. FWHM as a function of surface density for all low energy filters tested at 35kVp.

Figure 2 shows the SNR_{tc} as a function of surface density for low-/ high-energy tungsten spectra at 35/70kVp filtered with Pd-100 μm and Ce, Cu, Eu, Nd, Sm, Ho, Yb respectively, for a μC size of 200 μm. It is obvious that SNR_{tc} values were above the threshold only for Cu, Ho and Yb filters. Maximization of SNR_{tc} was accomplished at the surface density range between 0.4 and 0.55gr/cm^2. An SNR value of 3 is achieved for a μC size of 200 μm. Thus, a 200 μm microcalcification size was considered as the minimum detectable μC size in this study.

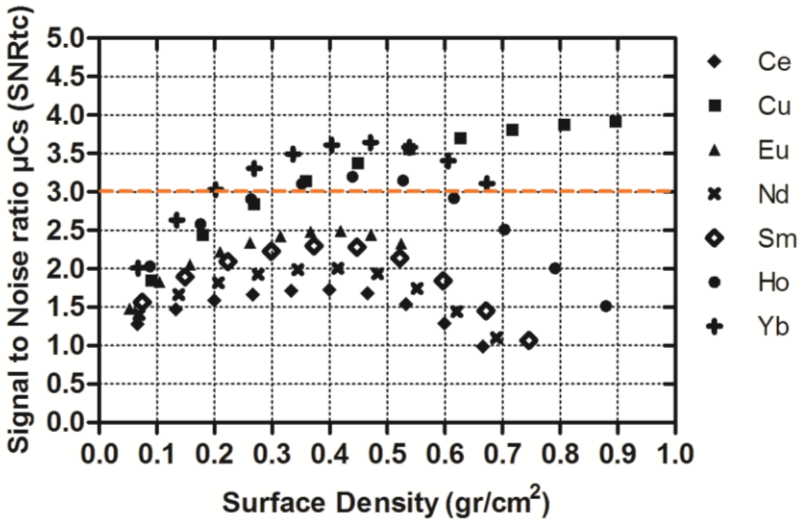

Figure 2. SNRtc as a function of surface density for 35kVp (LE) filtered with Pd-100 μm and 70kVp (HE) with all filters for μC size of 200 μm.

Figure 3 shows the entrance exposure as a function of surface density for low-/ high-energy tungsten spectra at 35/70kVp filtered with Pd-100 μm and all high energy filters, respectively. In the surface density range of 0.4 and 0.55gr/cm^2 only Ho and Yb filters are below the threshold of 6mGy. Note that Yb slightly minimizes entrance dose within this range. For this reason, Yb was considered to be the high energy filter.

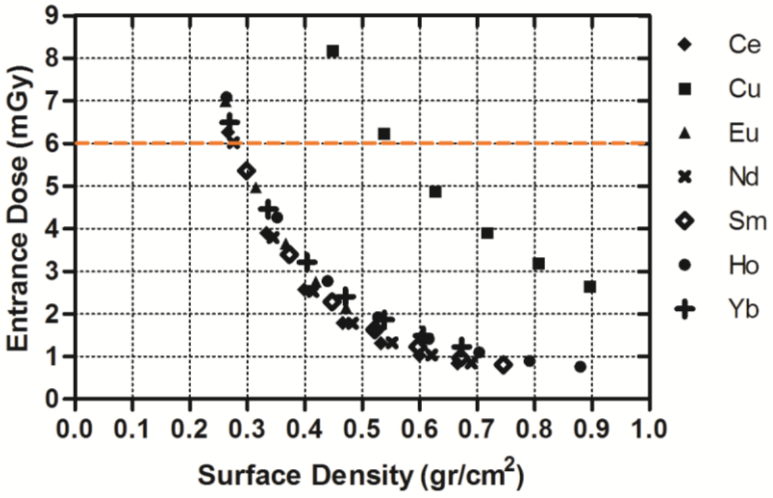

Figure 3. Entrance dose as a function of surface density for 35kVp (LE) filtered with Pd-100 μm and 70kVp (HE) with all filters.

4. Conclusion

In this simulation study, a prototype dual energy mammography system was modelled, using a CMOS based imaging detector with different X-ray tungsten spectra. Optimization was based on the maximization of SNR_{tc} while minimizing the entrance dose. The best compromise between SNR_{tc} value and dose was provided by 35kVp with added beam filtration of 100 μm Pd and 70kVp Yb filtered spectrum of 800 μm for the low and high energy, respectively. Computer simulation results show that a SNR_{tc} value of 3.6 can be achieved for a calcification size of 200 μm and assuming a 50% adipose and 50% glandular tissue composition and a breast thickness of 5 cm. The total entrance dose was 1.85mGy. Compared with previous studies, this method can improve detectability of microcalcifications.

Acknowledgement

This research has been co-funded by the European Union (European Social Fund) and Greek national resources under the framework of the "Archimedes III: Funding of Research Groups in TEI of Athens" project of the "Education & Lifelong Learning" Operational Programme.

5. References

[1] Wagner F and Brown G 1985 *Phys. Med. Biol.* **30** 489
[2] Brandan M and Ramirez V 2006 *Phys. Med. Biol.* **51** 2307
[3] Shaw C and Gur D 1991 *J. Digit. Imaging* **5** 262
[4] Lemacks M, Kappadath S, Shaw C, Liu X, Whitman G 2002 *Med. Phys.* **29** 1739
[5] Kappadath S and Shaw C 2003 *Med. Phys.* **30** 1110
[6] Kappadath S and Shaw C 2004 *Phys. Med. Biol.* **21** 2563
[7] Kappadath S and Shaw C 2008 *Phys. Med. Biol.* **53** 5421
[8] Ducote J and Molloi S 2008 *Med. Phys.* **35** 5411
[9] Boone J, Fewell T and Jennings R 1997 *Med. Phys.* **24** 1863
[10] Boone J and Seibert A 1997 *Med. Phys.* **24** 1661
[11] Koukou V, Martini D, Sotiropoulou P, Fountos G, Michail C, Valais I, Kandarakis I and Nikiforidis G 2012 *e-JST* **7** 79
[12] Michail C, Spyropoulou V, Fountos G, Kalyvas N, Valais I, Kandarakis I and Panayiotakis G 2011 *IEEE Trans. Nucl. Sci.* **58** 314
[13] Hubbell J and Seltzer S 1995 US Department of commerce NISTIR 5632
[14] Koukou V, Martini N, Fountos G, Sotiropoulou P, Michail C, Valais I, Kandarakis I and Nikiforidis G 2014 *IFMBE Proceedings* **41** 459
[15] Hammerstein R, Miller D, White D, Masterson M, Woodward H and Laughlin J 1979 *Radiology* **130** 485
[16] Gong J, Arnold J and Cohn S 1964 *Anat. Rec.* **149** 319
[17] Seferis I, Michail C, Valais I, Fountos G, Kalyvas N, Stromatia F, Oikonomou G, Kandarakis I, Panayiotakis G. 2013 *Nucl. Instrum. Meth. Phys. Res. A*.**729** 307
[18] Michail C, Fountos G, Liaparinos P, Kalyvas N, Valais I, Kandarakis I and Panayiotakis G. 2010 *Med. Phys*. **37** 3694